The muon spin response to intermittent hyperfine interaction: modelling the high-temperature electrical activity of hydrogen in silicon

2004 J. Phys.: Condens. Matter 16 S4739

(http://iopscience.iop.org/0953-8984/16/40/017)

INSTITUTE OF PHYSICS PUBLISHING JOURNAL OF PHYSICS: CONDENSED MATTER

J. Phys.: Condens. Matter **16** (2004) S4739–S4760 PII: S0953-8984(04)84617-4

The muon spin response to intermittent hyperfine interaction: modelling the high-temperature electrical activity of hydrogen in silicon

J S Lord[1], S F J Cox[1,2,6], M Charlton[3], D P Van der Werf[3], R L Lichti[4] and A Amato[5]

[1] ISIS Facility, Rutherford Appleton Laboratory, Chilton OX11 0QX, UK
[2] Department of Physics and Astronomy, University College London, WC1E 6BT, UK
[3] Department of Physics, University of Wales Swansea, Singleton Park, Swansea SA2 8PP, UK
[4] Department of Physics, Texas Tech University, Lubbock TX 79409-1051, USA
[5] Paul Scherrer Institute, Laboratory for Muon-Spin Spectroscopy, CH-5232 Villigen PSI, Switzerland

Received 5 April 2004
Published 24 September 2004
Online at stacks.iop.org/JPhysCM/16/S4739
doi:10.1088/0953-8984/16/40/017

Abstract

At temperatures above 600 K in silicon, unlike at lower temperatures, the partitioning of muonium between its neutral paramagnetic states and its charged or electronically diamagnetic states corresponds closely to thermodynamic equilibrium. The individual charge states are short lived, with many cycles of carrier capture and release occurring within the muon lifetime. The resultant intermittent hyperfine interaction depolarizes the muons strongly, with longitudinal and transverse relaxation rates remaining distinct up to about 700 K but becoming equal at still higher temperatures. Data up to 900 K are presented and interpreted. The muon spin rotation spectrum in transverse magnetic fields, although collapsed to a single broad line in this charge exchange regime, is shifted substantially from the muon Larmor frequency, the shift being non-linear in field and only in small part due to electron polarization. A new density matrix treatment shows how all three observables can be accounted for with a consistent set of transition rates. These in turn may be interpreted in terms of effective donor and acceptor energy levels appropriate to this high-temperature regime, confirming negative-U behaviour and providing the first estimate, for muonium, of this elusive parameter. At temperatures where passivation complexes are dissociated, these findings provide a guide to, and microscopic models for, the electrical activity of hydrogen.

[6] Address for correspondence: ISIS Facility, Rutherford Appleton Laboratory, Chilton OX11 0QX, UK.

1. Introduction

1.1. Muonium as an experimentally accessible model for hydrogen

Muonium in silicon is treated in this paper from the perspective of a very real materials science issue, namely the electrical activity of hydrogen impurity [1]. We review how μSR discoveries have contributed to the current understanding of the underlying interplay of site and charge state and examine the extent to which the analogy between muonium and hydrogen itself has been validated at temperatures below and around room temperature. We go on to show how μSR studies are illuminating processes which become active at high temperature, with data up to 900 K. This work is concerned with the isolated or monatomic defect centres, namely the interstitial proton or positive muon, the neutral hydrogen or muonium centres and, where appropriate, the hydride ion and its muonium counterpart. At ordinary temperatures these will be quite rare for hydrogen itself, most of this unavoidable but highly reactive impurity being paired with other defects or impurities. They will become more important at high temperatures, where passivation complexes are dissociated—typically above 400 K for donor complexes and 500 K for shallow acceptors [1]. But then the individual charge states are short lived, as we see in the later sections of this paper. For these various reasons the isolated centres have been hard to detect or characterize by conventional spectroscopies for hydrogen itself. The microsecond timescale of μSR observations on the other hand, set by the muon lifetime, $\tau_\mu \approx 2.2\ \mu$s, greatly favours observation of isolated states of muonium in intrinsic interstitial sites. The nature of muon spin relaxation—in particular, the response to intermittent hyperfine interaction which is the topic of this paper—additionally allows inferences to be drawn on processes such as charge state transitions which occur on much faster timescales still. In the present work, we infer charge state lifetimes as low as a few picoseconds.

1.2. The neutral paramagnetic centres

For the neutral centres, which are paramagnetic by virtue of a single unpaired electron, it is no exaggeration to say that the much needed microscopic pictures of crystallographic site and electronic structure came first from muonium spectroscopy. The discovery of their metastability in Si is already some three decades old: figure 1 reproduces the original spectrum due to Brewer *et al* [2], showing hyperfine signatures of two distinct states coexisting in a μSR spectrum of Si recorded at cryogenic temperature. The details and implications of their interpretation, as well as those of similar spectra in Ge, diamond, GaAs and GaP, have since been reviewed extensively [3, 4] and [5][7]. In brief, their assignment to cage-centred and bond-centred interstitial states with very different electronic structures has subsequently been ratified by the modelling techniques of computational chemistry, as well as by such spectroscopic data as exist for hydrogen itself. Several surprises were involved here. The first is that, unlike the interstitial Li^+ ion, the interstitial positive muon does not form a shallow centre in which an electron is weakly bound, in an orbital which is dilated both by the low effective mass of conduction electrons and by the bulk dielectric constant of silicon. Instead, both muonium states are deep, with thermal stabilities indicating more tightly bound electrons and with hyperfine parameters indicating correspondingly compact electronic orbitals.

The cage-centred neutral state resembles atomic muonium, in that it has an isotropic hyperfine constant and so is spherically symmetric. Trapped-atom states of interstitial hydrogen are well known to ESR spectroscopy in certain oxides and halides (i.e. in dielectrics)

[7] This summary description cites earlier reviews of muonium spectroscopy and introduces spin exchange and charge exchange dynamics.

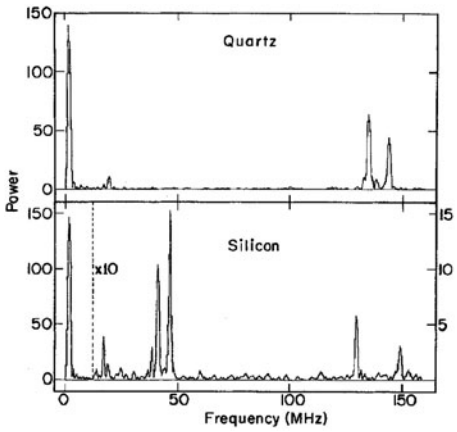

Figure 1. The original muon spin rotation spectra for silica and silicon [2], the former showing a signature of interstitial atomic muonium, the latter showing both cage-centred and bond-centred states.

and figure 1 shows that there is such a state of muonium in silica, SiO_2. ESR spectroscopy fails to detect atomic hydrogen centres in elemental Si, however, or indeed in other tetrahedral semiconductors, so there is an apparent contradiction with the μSR finding here. (We argue that the μSR spectroscopy is valid, and provides unique insights into hydrogen states that are simply too reactive or transient to be seen by ESR spectroscopy.) A second surprise was that this seemingly atomic state of muonium in Si has a hyperfine constant ($A = 2006$ MHz at low temperatures) which is scarcely half that of free or vacuum state atomic muonium (4463 MHz), as though its 1s orbital only had 45% occupancy. Despite this evident chemical interaction with the surrounding host atoms, there is no directional bonding; the elastic interaction must also be minimal, since this quasi-atomic form of muonium is highly mobile at all temperatures for which its spectrum is visible (up to about room temperature). While this was originally dubbed 'normal muonium', we follow the recent usage and designate this state as Mu^0_T, emphasizing its charge state as well as its effective location at the 'T site', i.e. the centre of the tetrahedral interstitial cages of the diamond-type lattice.

Arguably the greatest surprise was the coexistence of the additional paramagnetic state of muonium in Si, at first dubbed 'anomalous muonium' or Mu^* but now designated Mu^0_{BC} following assignment of the muon site to the centre of a stretched Si–Si bond (BC = bond centre). Originally quite unanticipated, it is now generally held to be the more stable of the two neutral centres, corresponding to the ground state of interstitial hydrogen. This is the conclusion of most calculations which take due account of the lattice relaxation, if not of the lattice vibration. Certainly there is a rather fine energy balance between the T and BC sites and in the present work we again question which lies lower. The unpaired electron wavefunction of Mu^0_{BC} has donor character, borrowing silicon antibonding orbitals [6–8], but it is a deep donor, detached from the conduction band by the local distortion, i.e. by the bond extension necessary to accommodate the muon. Accordingly, its characteristic hyperfine frequencies disappear from the μSR spectra above about 150 K, as this species appears to ionize. (We discuss below whether this is literally the loss of an electron to the conduction band or whether the higher temperatures inhibit electron capture in the first place.) The hyperfine anisotropy indicates that it remains totally immobile up to this temperature, self-trapped by the lattice relaxation, which entails a stretching of the original Si–Si bond by some 40%. The ionization

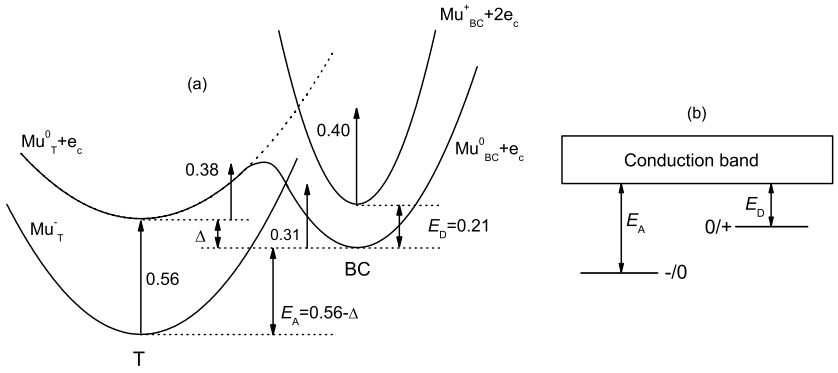

Figure 2. Muon sites and energy levels in silicon, showing the correspondence between (a) the configuration diagram [11] and (b) the donor and acceptor levels relative to the band gap [23].

energy is 210 meV, as determined from RF muon spin resonance [9–11], and is taken as defining the depth of a donor level below the conduction band.

For comparison, the donor depth is only 34 meV for interstitial Li and 46 meV for the classic shallow donor, substitutional P, both of which are essentially fully ionized by about 50 K [12]. Although both Mu^0_T and Mu^0_{BC} show varying degrees of delocalization of the unpaired electron onto the surrounding lattice, in neither is it anything like that appropriate to effective-mass donors: by contrast, the hyperfine constant is reduced by a factor of order 10^4 to just a few hundred kilohertz for the shallow-donor muonium states recently discovered in certain compound semiconductors [13, 14].

1.3. The charged diamagnetic centres and the interplay of site and charge state

Just above the Mu^0_{BC} ionization temperature, i.e. above about 150 K, the corresponding positive ion is assumed also to be located at the bond centre, in an electronically diamagnetic state which we designate as Mu^+_{BC}. We use this explicit nomenclature, reserving μ^+ for the energetic incoming muons, to emphasize the fact that muons, like protons, cannot remain as free particles in condensed matter. They always seek out the region of highest electron density to minimize the defect energy, here the spin-paired electron cloud of the valence bond. Although there is no experimental site determination for Mu^+ in Si, nuclear magnetism being too weak to give the necessary signature, the BC site is the theoretical expectation for H^+ [15]. That Mu^+_{BC} remains the chief diamagnetic muonium state up to at least 400 K is a reasonably safe assumption and we shall argue that it remains so to much higher temperatures.

The hydride ion, on the other hand, believed to exist in sufficiently n-type material, is repelled to the region of lowest electron density, which in Si is the T site cage centre [15], thus H^-_T. In semiconductors with abundant nuclear moments, especially the quadrupolar moments carried by group III and group V nuclei, site determinations for the diamagnetic charged centres are more explicit: both Mu^+_{BC} and Mu^-_T have been identified experimentally in GaAs [16, 17].

The relationship between site and charge state is summarized in figure 2(a), with relative energy levels and barrier heights as deduced from radio-frequency muon spin resonance (RF-μSR) experiments performed at TRIUMF up to 450 K [9–11]. A closely similar scheme is commonly used for hydrogen, with analogous nomenclature designating the site and charge state [18]. The relative energy levels, barrier heights and dynamical parameters all prove to be remarkably similar for muonium and hydrogen in silicon (in so far as they are known

for hydrogen), justifying the use of muonium data as a guide to the electrical activity of hydrogen [9, 10, 18].

Note that in order to compare the relative energies of different muonium charge states, the overall system (e.g. in a cluster calculation) must have the same total number of electrons. Thus in figure 2(a), the Mu^0 energies include that of one electron at the conduction band minimum, and those of Mu^+ include two, for comparison with Mu^-. This convention tends to conceal the fact that the ionic energies vary with the Fermi energy and to give a false impression of their relative energies. For instance, giving the energies of the additional electrons a mid-gap Fermi energy rather than setting them in the conduction band inverts the order of the ionic levels, making Mu^+_{BC} thermodynamically the most stable state and Mu^-_T the least stable, as we believe to be the case in undoped material. We give a different representation in figure 6 below, when calculating equilibrium occupancies.

Although some authors question the importance of H^0_T, finding that there is no adiabatic barrier between the T and BC sites [21], for others it is the elusive transport states of hydrogen [18]. The T to BC barrier could well be dynamic in origin, the heavy Si atoms responding only sluggishly to the instantaneous position of an approaching hydrogen atom [19], or of a still lighter muonium atom ($m_{Mu}/m_H \sim 1/9$). The mobility of H^0_T would certainly explain its ESR silence, since on the ESR timescale it would seek out and react with other defects and impurities. The so-called AA9 centre of hydrogen in silicon, found by ESR spectroscopy [20] shortly after elucidation of the Mu^0_{BC} structure [6], could immediately be identified as H^0_{BC}, its hyperfine parameters (after scaling with the ratio of the muon and proton magnetic moments) being essentially identical.

1.4. Electrical activity: donor and acceptor levels

Figure 2(b) gives the correspondence with the electrically active donor and acceptor levels. If Mu^0_{BC} is indeed the more stable of the two neutrals, construction of the donor level is straightforward: its depth below the conduction band is then the ionization energy, without site change, of Mu^0_{BC}. The corresponding value for hydrogen, deduced from deep-level transient spectroscopy, has most recently been given as 175 meV [18]. The difference between the muonium and hydrogen values is quite accurately accounted for by the different zero-point energies of the muon and proton, in the appropriate potential wells [14]. The zero-point energy is not shown in figure 2 but it amounts to several hundred meV for the muon—greater than for the proton by a factor $\sqrt{m_H/m_{Mu}} \approx 3$. Fortunately, the electrically active levels of figure 2(b) represent differences between energy levels in figure 2(a), so the isotope effects are relatively small, as quantified elsewhere [14]. It is this that makes muonium a useful model for the electrical activity of hydrogen. It is worth noting that, for H^0_{BC} as for Mu^0_{BC}, the vibrational energy quantum (twice the respective zero-point energies, assuming a harmonic potential well) exceeds the binding energy of the unpaired electron [22]: roughly speaking, H^0_{BC} ionizes before it can be excited to its first vibrational level.

Construction of the acceptor level is more problematic. The original identification of its depth, again referred to the conduction band, as the ionization energy without site change of Mu^-_T [9], is only correct if Mu^0_T is the more stable neutral. Otherwise, the thermodynamic definition is the energy difference between the stable neutral and the stable negative ion, i.e. between Mu^0_{BC} and Mu^-_T, when these are ordered as in figure 2, and likewise for hydrogen [23]. The Mu^-_T ionization energy is experimentally the more accessible parameter, determined by radio-frequency resonance studies (RF-μSR) as 560 meV, but from this must be subtracted the site change energy Δ between Mu^0_T and Mu^0_{BC} [11].

1.5. The negative-U question

So far, this crucial site change energy Δ—not the barrier between the T and BC sites but the difference between the two potential minima—has eluded experimental determination. This has made the ordering of the donor and acceptor levels indeterminate for muonium in silicon, although we attempt a resolution in the present work. It brings us to a matter of some interest for hydrogen itself. The donor level can be identified with the value of the Fermi energy at which the neutral centre and positive ion are in equilibrium, i.e. the $0/+$ switching point. The acceptor level likewise concerns equilibrium of the neutral centre and the negative ion, i.e. the $-/0$ switching point. This nomenclature is used in figure 2(b) and is explicit in figure 6 below. Hydrogen in silicon is now generally considered to constitute a so-called negative-U defect, in which the $0/+$ switching level lies above the $-/0$ level. (Here U is the Hubbard or Anderson correlation energy, in which Coulomb repulsion of two electrons in a doubly occupied state, itself always positive, is offset by lattice relaxation energies.) With single-site ionization energies for Mu^0_{BC} and Mu^-_T of 210 and 560 meV, respectively, Hitti *et al* note that U is negative only if $\Delta < 350$ meV [11]. Tantalizingly, early theoretical estimates vary widely [24] and it is now realized that vibrational entropies may introduce a temperature dependence of the levels [25]—or even a possible inversion, as our own data suggest. For a positive-U system, the $0/-$ switching level lies above the $0/+$ level, so as the Fermi energy is raised through the gap, the positive, neutral and negative charge states are stabilized in turn. If muonium in silicon does indeed constitute a negative-U system, thanks essentially to the different lattice sites adopted by the positive and negative ions, this order is inverted so there is no position of the Fermi level for which neutral centres are thermodynamically stable, either at the cage-centred or the bond-centred state. Yet both are observed, coexisting in the low-temperature spectra, with spin states that are long lived on the microsecond μSR timescale. Of course, muonium centres are never formed in sufficient concentration (even at a pulsed muon source) to equilibrate amongst themselves. Otherwise the implication of negative U is that they would disproportionate, according to

$$2Mu^0 \rightarrow Mu^+ + Mu^-.$$

The fact that the neutral paramagnetic AA9 centre, i.e. H^0_{BC}, is only detectable by means of ESR under conditions of band-gap illumination [20] is entirely consistent with negative-U behaviour.

The process of muon implantation, which must include the generation of electron–hole pairs as the incoming energy is dissipated, appears to favour formation of the neutral centres, which we take to be the starting point for subsequent charge state transitions. Muonium dynamics, then, usually displays the initial stages of approach to thermodynamic equilibrium. Thus the Mu^0_{BC} spectrum in Si disappears by broadening in the ionization regime [3], as though a single electron is first captured whatever the temperature, but the neutral state lifetime is subject to an Arrhenius law. The ionization process may even be displayed directly by RF final state analysis in a narrow temperature range [26]. It remains to reconcile this model, however, with indications of a small but measurable delay to the initial electron capture, both in Si [27] and, more convincingly, in GaAs [28].

According to figure 2(a), disappearance of the Mu^0_T spectrum around room temperature would correspond to a thermally induced site change to the bond centre (the barrier is 380 meV), followed by rapid ionization. We should consider whether it might instead be due to hole ionization, $Mu^0_T \rightarrow Mu^+_T + h$, but the low ionization energy would be incompatible with the general consensus [11, 21] that the acceptor level lies around mid-gap (the band gap is close to 1.1 eV in Si at room temperature). We are also able to exclude hole ionization, even at higher temperatures, from our own measurements (see section 7). Several more alternative

explanations should be considered, according to the authors of the model of delayed muonium formation [27, 28]: if the electron is initially captured into excited or Rydberg orbitals, thermal ionization of these weakly bound precursor states may simply prevent their cascade to the Mu^0_T state above room temperature. We see below, however, that this cascade is certainly not completely forbidden, even at much higher temperatures. Alternatively, second electron capture may convert Mu^0_T to Mu^-_T—a process which is undoubtedly important in n-type Si [11] and possibly also in intrinsic material at higher temperature.

1.6. The charge exchange regime

We come now to the exploration of these higher temperatures, with data up to 900 K. Just above room temperature, a single narrow line at the muon Larmor frequency is seen in the muon spin rotation spectrum, presumed to correspond to the positive ion, Mu^+_{BC}. Full asymmetry is not recovered until higher temperature is reached [3] but any muonium state is too short lived to be characterized. The line remains narrow until just above 400 K, when it begins to broaden, accompanied by the onset of a similar muon spin relaxation in longitudinal field. The longitudinal relaxation was studied in some detail at TRIUMF by Chow et al [29], who attributed it to a charge exchange regime in which conduction electrons are repeatedly trapped and released by the implanted muons. In effect, muonium is formed and reionized repeatedly when the encounter with thermally excited intrinsic carriers is sufficiently frequent. This was an important insight, identifying processes for muonium which have their counterparts in the high-temperature electrical activity of hydrogen.

The charge exchange process may be compared and contrasted with that of spin exchange, where a paramagnetic centre remains undissociated but has its electron spin frequently flipped by close encounters, i.e. Heisenberg exchange, with passing conduction electrons, usually extrinsic. In Si, spin exchange is visible for Mu^0_{BC} below the relevant ionization temperature in highly doped n-type samples [30]. A mathematical treatment of fast spin exchange for muonium centres or muoniated radicals with anisotropic hyperfine interactions is given by Senba [31]. Both charge and spin exchange can in principle involve holes as well as electrons and we return below to the question of which carriers dominate. Examples of all the various processes are seen in the effects of encounters with optically excited carriers [32, 33]. In principle, comparison of the muon response to doping, illumination or heating can distinguish majority and minority carrier processes. Extending models of the type introduced by Kreitzman *et al* [9], the recent paper by Kadono, Macrae and Nagamine [34] gives a useful compendium of the different processes which must be considered, involving both electrons and holes[8], as well as the different signatures in the μSR data by which they may be recognized. It remains to be demonstrated, however, that the expressions introduced by these various authors for site and charge state transitions do lead, in detailed balance, to the expected populations of each state in the final thermodynamic equilibrium.

1.7. A two-state model

Confining our attention to the encounters with thermally excited carriers, quite strong muon spin relaxation is induced by the resultant intermittent hyperfine interaction. Measured in low longitudinal field for nominally pure or undoped Si, the relaxation rate peaks at some 25 μs^{-1}

[8] Note, however, that in expressions of the type $nv\sigma$ for carrier capture rates (i.e. number density × velocity × cross-section) it is not the Fermi velocity that should be used but the thermal velocity, as appropriate to carriers at their respective band edges (e.g. electrons at the conduction band minimum). Fermi velocity is not an appropriate concept for non-metals.

around 600 K. It also requires high magnetic fields to quench the relaxation and from the form of the field dependence Chow *et al* [29] were able to show that the hyperfine constant involved corresponds to that of Mu_T^0 rather than that of Mu_{BC}^0: the inferred values fit well to an extrapolation of values determined spectroscopically [3] up to room temperature. By implication, Mu_T^0 can reach its $n = 1$ ground state momentarily following electron capture, even at elevated temperatures. This is not to say that Mu_{BC}^0, or excited states of Mu_T^0, are not also involved in charge exchange cycles but simply that, if so, they are too short lived for the muon spin to respond to their contribution.

Simplifying the problem to a two-state model, i.e. an interplay between the cage-centred neutral atom and a charged diamagnetic state, Chow *et al* [29] deduced a time-average occupancy of the Mu_T^0 state, i.e. a neutral fraction, rising to 6% at 800 K. Noting that the onset temperature for relaxation shifts to higher temperature with p-type doping, these authors further identified the charge cycle as a capture and loss of electrons, with an effective 0/+ transition located in the upper half of the energy gap, 340 meV below the conduction band. They gave two possible interpretations. In one, they invoked a breakdown of adiabaticity and surmise that the muon is unable to access the bond centre at high temperatures. The effective donor depth is then unrelated to the scheme of figure 2. In the alternative, the fitted energy of 340 meV was identified as the activation energy for the process

$$Mu_T^0 \rightarrow Mu_{BC}^+ + e,$$

close to the barrier to site change entered as 380 meV in figure 2 (this latter determined from RF-μSR data around 400 K [9, 11]). In our view, the first interpretation is untenable, since it is tantamount to identifying the activation energy with the direct ionization energy of Mu_T^0, without site change. Given the muonium hyperfine constant, which at 600 K is inferred to be around 40% of the free atom value, the corresponding electron binding energy must be a substantial fraction of a Rydberg[9]. The $(0/+)_T$ switching level is not represented in figure 2(b) but it cannot lie within the gap: we would draw it very much deeper, e.g. below the valence band.

2. Experiment: the three observables

2.1. Longitudinal and transverse relaxation

In our own experiments, working on the GPS instrument at PSI [35] with partial spin rotation of the πM3 muon beam, we were able to make simultaneous measurements of the transverse and longitudinal responses at each temperature. Examples of the temperature dependences are shown in figures 3 and 4. The sample used here, and for all the measurements presented in the present paper, is a lightly doped (10^{14} cm^{-3}) p-type one. It is in fact the same sample as was designated P14 by Kreitzman *et al* [9] and used in their RF resonance experiments. The longitudinal relaxation data are similar but not identical to those reported earlier by Chow *et al* [5] and Cox *et al* [36] for the nominally undoped silicon sample denoted as P12 (having a net acceptor concentration of $\sim 10^{12}$ cm^{-3}), the onset of relaxation being shifted to slightly higher temperatures.

In the new measurements it is clear that the two relaxation rates, longitudinal and transverse, differ on the low-temperature side of their peaks. This deserves some comment: it is common in magnetic resonance, especially in NMR (nuclear magnetic resonance), to

[9] A Rydberg, $Ry = 13.6$ eV, is the binding or ionization of hydrogen in its free or vacuum state. That of free muonium is the same to within a quarter per cent, being a simple function of the reduced electron mass. No simple formula relates binding energy to hyperfine constant for Mu_T^0 in Si, nor for quasi-atomic normal muonium in other materials, since effective-mass theory clearly does not apply to such compact, strongly bound interstitial states.

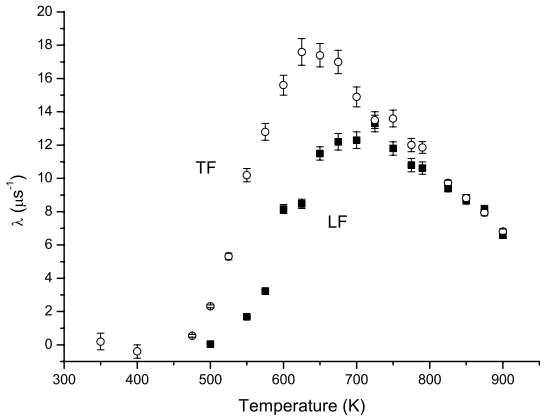

Figure 3. The temperature dependence of the two muon spin relaxation rates, measured in transverse and longitudinal fields (TF and LF), both of 0.2 T [36].

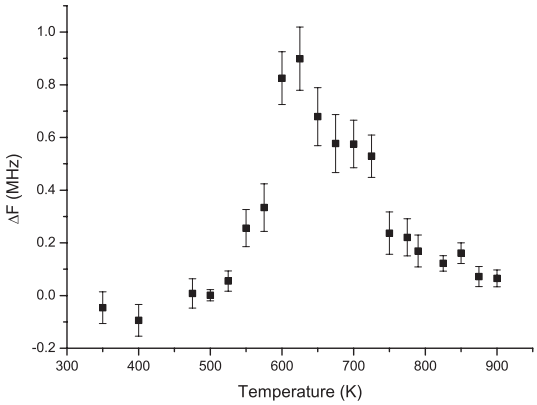

Figure 4. The temperature dependence of the shift of the muon spin rotation frequency, relative to the muon Larmor frequency. This data set is for a field of 0.2 T, where the Larmor frequency is 27.20 MHz [36].

observe a peak in longitudinal relaxation rate or, equivalently, a so-called T_1-minimum. It is also common in NMR to find that the transverse relaxation time, designated T_2, differs from the spin–lattice relaxation time T_1 in the slow fluctuation regime but becomes equal to it in the fast fluctuation regime. This behaviour is superficially similar to that shown by the present μSR data but the analogy is not exact, since in the present case T_2 is undefined in the static limit, where hyperfine interactions would lead to a splitting rather than a simple broadening of the spectrum. More analogous to the present case is that of spin exchange on an otherwise long-lived paramagnetic centre. The transverse and longitudinal relaxation rates are then also different in the slow fluctuation regime but peak and become equal when the spin exchange rate becomes comparable with hyperfine constant [39].

For the present case of charge exchange there are two transition rates to consider and it is the exit rate from the paramagnetic state relative to its instantaneous hyperfine constant that controls this behaviour. For a complete description we must extract the separate transition rates for entry into and exit from the neutral paramagnetic centre. This we do from simultaneous fits to field dependences of the two relaxation rates, together with a third observable, which we now

introduce. A preliminary account of this work has been given in a conference presentation [38]; in sections 3–8 we give a fuller account, both of the new simulation and fitting methods and of the discussion of results.

2.2. The paramagnetic shift

While the fluctuating component of an intermittent hyperfine interaction depolarizes the muon spin, its time average must represent an effective field, which shifts the Larmor precession frequency from its free muon value, $f_\mu = \frac{1}{2\pi}\gamma_\mu B$. (The muon gyromagnetic ratio is usefully expressed as $\frac{1}{2\pi}\gamma_\mu = 136\,\mathrm{MHz\,T^{-1}}$, so, for comparison with the data of figure 4, for instance, the Larmor frequency is 27.2 MHz at 0.2 T.) In the limit of fast transition rates, and for an isotropic contact interaction A, in units of frequency, we expect [36]

$$\delta f = \tfrac{1}{2} A p_\mathrm{e} p_0, \tag{1}$$

or, equivalently, a proportional shift of

$$\frac{\delta f}{f_\mu} \approx \frac{hA}{4kT}\frac{\gamma_\mathrm{e}}{\gamma_\mu} p_0. \tag{2}$$

Here p_0 is the time-average neutral fraction and p_e the electron polarization, approximated in equation (2) by a Boltzmann expression appropriate to isolated paramagnetic centres. Seeking such a shift in these terms, Cox *et al* [36] found it to be surprisingly large. Measured at PSI in 0.6 T (for the same undoped silicon sample P12 as was used at TRIUMF by Chow *et al*), it was found to reach 0.6% around 600 K, close to the temperature where the relaxation rate is maximal. Setting this value in equation (2) gives $p_0 \approx 1$, i.e. appears to require a neutral fraction close to unity at these temperatures. This is thermodynamically impossible in a two-state (0/+) model but, coincidentally, could be reconciled with an interplay of three of the four states of figure 2, namely between Mu^0_T, $\mathrm{Mu}^0_\mathrm{BC}$ and $\mathrm{Mu}^+_\mathrm{BC}$. A bottleneck to site change artificially enhances the time-average occupancy of Mu^0_T in this restricted scheme, although in the full four-state model the neutral fraction is limited to low values by transitions to Mu^-_T. No set of transition rates could be found which consistently explained both the frequency shift and the longitudinal relaxation data. A similar discrepancy between the relaxation data and RF resonance data, notably for p-type samples, led Hitti and Kreitzman [37] to introduce intermediate excited states in their model of the electron capture process.

A resolution of the puzzle came with further work by Cox *et al* [38], who found that the frequency shift is not linearly proportional to the applied field, as implied by equation (1). (In other words, the proportional shift is not field independent, as in equation (2).) Electron polarization, which is undoubtedly proportional to field at high temperatures, is not the dominant origin of the frequency shift. Instead, the shift must originate in the time dependence of the hyperfine interaction, rather than its static average. The field dependences are shown analysed in figure 5 below, after an exposition of the theory in section 3. Figure 4 shows the temperature dependence of the shift, measured at 0.2 T for the new sample.

It is helpful to regard the broad single-line precession spectrum as the dynamical average of the four contributing frequencies from each short-lived paramagnetic state, i.e. of the allowed transitions between the Breit–Rabi eigenstates, mixed with the pure Larmor precession signal of the diamagnetic states. However, only in the limit of short muonium charge state or electron spin state lifetimes do these collapse to their algebraic average, slightly offset from the muon Larmor frequency as in equations (1) and (2). In the regime where the spin or charge state transition rates are comparable with the contributing frequencies, or rather their differences, their averaging is a more complex problem. Numerical simulations due to Senba [39], for the case of spin exchange on muoniated radicals, indicate the possibility of more substantial

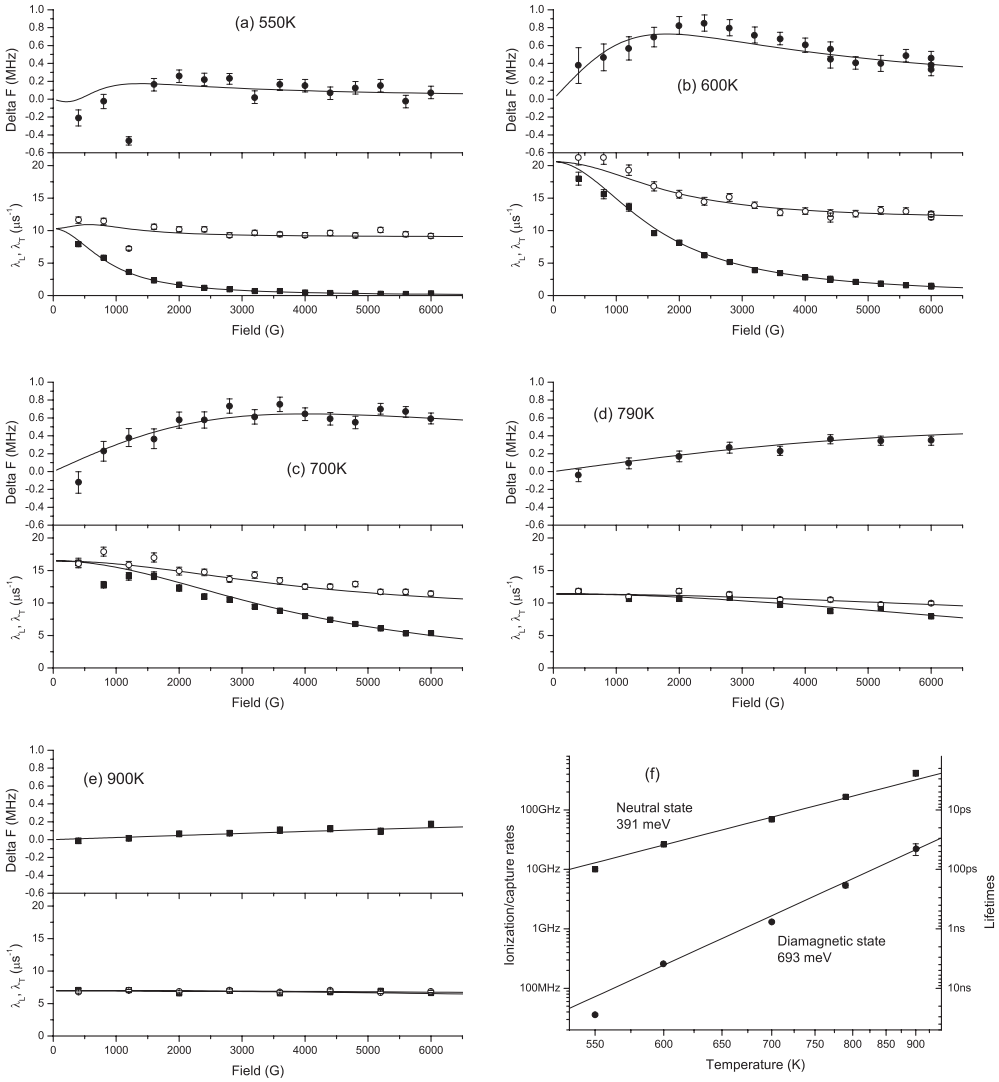

Figure 5. For data sets at each temperature ((a)–(e)), simultaneous or global fits are shown for (■) longitudinal relaxation, (○) transverse relaxation and (●) frequency shift as a function of field. The resultant variation with temperature of the fitted transition rates is shown in (f) and tabulated in table 1.

shifts from the muon Larmor frequency. An analytical expression is given by Gorelkin *et al* [40], derived for spin exchange on muonic atoms, i.e. for the shift from the Larmor frequency of negative muons, and including both dynamic and Boltzmann terms. Inserting parameters appropriate to positive muons and muonium in silicon, this expression describes the qualitative field dependence of our data quite well; on scaling by neutral fraction to adapt it to charge exchange, however, it fails to account for the absolute magnitude of the shift.

We have therefore resorted to direct numerical simulations of muon response in the charge exchange regime, as described in the following section. The new method allows simultaneous fitting of all three observables, namely the transverse field frequency shift and the relaxation rates measured in both transverse and longitudinal field.

3. Theory

The calculation of the spin evolution is based on the density matrix method, where the density matrix ρ is defined such that

$$\mathrm{d}\rho/\mathrm{d}t = [H, \rho], \tag{3}$$

$$\langle X \rangle = \mathrm{Tr}(X\rho), \tag{4}$$

$$\mathrm{Tr}(\rho) = 1.$$

The diagonal terms $\rho_{i,i}$ give the probability that the system is in the basis state ϕ_i. Off-diagonal terms $\rho_{i,j}$ give the mixing between states i and j. If ρ is zero except for $\rho_{i,i} = 1$, then the system is definitely in basis state ϕ_i. If $\rho = \frac{1}{N}\mathbf{1}$ (i.e. the normalized unit matrix), the system is completely unpolarized. When ρ is written using the eigenvectors of the Hamiltonian H as basis states, its time evolution can be obtained from the set of equations

$$\rho_{i,i}(t) = \rho_{i,i}(0),$$

$$\rho_{i,j}(t) = \rho_{i,j}(0)\exp(\mathrm{i}(E_i - E_j)t/\hbar).$$

However, in the present work, we use equation (3) directly.

3.1. Spin flips

If there is a probability x of the spin flipping at time t, we can write

$$\rho(t+\epsilon) = (1-x)\rho(t-\epsilon) + x\rho'(t-\epsilon),$$

where ρ' is generated from ρ by flipping the spin. This is done by exchanging both columns and rows with spin up with the corresponding ones with spin down but other quantum numbers unchanged. The basis states used at this stage must have each spin as a good quantum number. Note that this spin flip rate x is half the 'spin encounter' or 'spin exchange' rate as a new spin being encountered may have the same spin as the one in the wavefunction. We can also write

$$\rho(t+\epsilon) = (1-2x)\rho(t-\epsilon) + 2x\rho_0(t-\epsilon),$$

where ρ_0 has the flipped spin polarization set to 0. It is possible to include a Boltzmann polarization of the new electron here.

If the spin may flip at any time with rate x per unit time, then

$$\mathrm{d}\rho(t)/\mathrm{d}t = -2x\rho(t) + 2x\rho_0(t).$$

3.2. Charge exchange or site change

We have a density matrix ρ_n for each charge state, normalized such that $\mathrm{Tr}(\rho_n)$ is the probability of the system being in state n. Since there is no 'mixing' between charge states we do not consider the state to be another quantum number. Any observable $\langle X \rangle = \mathrm{Tr}(X \sum \rho_n)$. For a charge state change from m to n at time t, probability x,

$$\rho_m(t+\epsilon) = (1-x)\rho_m(t-\epsilon),$$

$$\rho_n(t+\epsilon) = \rho_n(t-\epsilon) + x\rho_m(t-\epsilon)$$

and for site change at any time, with rate x per unit time,

$$\mathrm{d}\rho_m(t)/\mathrm{d}t = -x\rho_m(t),$$

$$\mathrm{d}\rho_n(t)/\mathrm{d}t = +x\rho_m(t).$$

All spins are assumed to be preserved in the change. Nothing happens to the overall measured signal $\mathrm{Tr}((\rho_m + \rho_n)\cdot\mathbf{S})$ until the states evolve differently with time.

The Hamiltonian for each state must include the same set of particles. If for example one state is ionized, the electron is still represented but its interaction with the other particles should be set to zero.

For repeated charge exchange either the same electron returns, having undergone no interaction except its own Zeeman splitting while ionized, or there is a new electron each time which is not spin polarized. This can be represented by giving the ionized electron a very high spin flip rate, or by including a spin flip with 50% probability in one of the charge exchange operations.

3.3. Solving the problem

Once all the interactions, spin flips and site changes have been included, we can evaluate $\mathrm{d}\rho/\mathrm{d}t$ for each element ρ_{ij} in the form $\sum \rho_{kl} X_{ijkl}$. Now we have an eigenvalue equation for the matrix $\mathbf{X}_{(ij),(kl)}$—but unlike in the usual quantum matrix method $\mathbf{X}$ is not Hermitian, so the eigenvalues may be complex. The solution is obtained in the form $\rho = \sum \rho_a \exp[(-\lambda_a + \mathrm{i}\omega_a)t]$ and then equation (4) is used to obtain the observable value such as the muon polarization.

4. Computation and data analysis

The logical sequence of program operations is described below. In practice some of these overlap, e.g. the static Hamiltonian is generated in block-diagonal form with each block being one charge state.

4.1. Static system

First calculate the Hamiltonian for each charge state, ignoring spin flips and charge exchange. For the case of $\mathrm{Mu}_{\mathrm{T}}^{0}$ in silicon we need only include the isotropic hyperfine coupling and Zeeman splitting of each spin, but in general the full anisotropic hyperfine interaction, dipolar interaction and quadrupole splitting could be added, governing the evolution:

$$\frac{\mathrm{d}\rho}{\mathrm{d}t} = [H, \rho] = H\rho - \rho H.$$

4.2. Flatten

Flatten the matrix ρ into a vector $\mathbf{R}$ and make a corresponding 'Hamiltonian' $\mathbf{X}$ such that we can write $\mathrm{d}\mathbf{R}/\mathrm{d}t = \mathbf{X}\mathbf{R}$, where $\mathbf{R}(i + N \times j) = \rho(i, j)$ and

$$\mathbf{X}((i + N \times j), (k + N \times l)) = H(i, k)\delta(j, l) - H(j, l)\delta(i, k).$$

4.3. Spin flip

Add spin flips for each state: we write the indices of the matrix $\mathbf{X}$ and the vector $\mathbf{R}$ as (ij, kl) where i and k represent the spin of the electron (row and column indices of the original ρ) and j and k represent all the other quantum numbers (the muon spin). Then

$$\mathbf{X}(ijkl, ijkl) = \mathbf{X}(ijkl, ijkl) - \lambda/2$$

along the diagonal and, elsewhere,

$$\mathbf{X}(ijkl, mjml) = \mathbf{X}(ijkl, mjml) + (\lambda/2) \times \beta(i, k).$$

Here $\beta(i, k)$ is the density matrix of the exchanging electrons—which could have non-zero polarization.

4.4. Combine charge states

Append the vectors $\mathbf{R}$ for each state to give a single long vector. Similarly join the matrices $\mathbf{X}$ to give a single matrix describing the evolution of either charge state, with the original matrices as block diagonals and the off-diagonal blocks set to zero.

4.5. Charge exchange

Now we add charge or site exchange. For diagonal elements of charge state i, subtract the sum of the rates of transition out of state i. Given $\mathbf{X}_{ij,kl}$ where i and k are the charge states and j and l are the quantum numbers within each state,

$$\mathbf{X}_{ij,ij} = \mathbf{X}_{ij,ij} - \sum_k \lambda_{ik}.$$

For the 'diagonal' elements of the off-diagonal blocks joining state i to k we add the rate of transition from i to k:

$$\mathbf{X}_{ij,kj} = \mathbf{X}_{ij,kj} + \lambda_{ik}.$$

Given the charge exchange rates in each direction, the equilibrium population can be calculated and may be used as the initial condition. Similarly, though only for a two-state system, given an overall charge cycling rate and populations for each state, the individual rates can be calculated.

4.6. Matrix solution

The final matrix equation is

$$\mathrm{d}\mathbf{R}/\mathrm{d}t = \mathbf{X}\mathbf{R}.$$

This is like the usual matrix equation for simple quantum mechanics, except that the eigenvalues are complex. Solve with a suitable numerical library subroutine to give:

- Purely imaginary eigenvalues: oscillating term, no relaxation. These must occur in conjugate pairs.
- Purely real, negative eigenvalues: 'longitudinal' relaxation.
- A complex, negative real part: damped oscillations. In conjugate pairs.
- The zero eigenvalue: non-relaxing polarization. One such state should have the 'flattened unit matrix' as its eigenvector meaning that the unpolarized state is stable. (The actual value may be different, if a non-zero spin flip polarization was used, or the equilibrium populations of the charge states are not equal.) There may be additional zero eigenvalues, for example in the case of no charge exchange.
- No eigenvalue should have a positive real part, which would imply exponentially increasing polarization with time.

Solutions will be of the form

$$\mathbf{R} = \sum \mathbf{R}_i \exp(E_i t)$$

and, after matching up conjugate pairs,

$$\mathbf{R} = \sum \mathbf{R}_i \exp(-\lambda_i t) \cos(\mathrm{i}\omega_i t + \phi_i).$$

In practice there is no need to match pairs, and this can cause difficulty when two pairs of levels are degenerate. We continue to use complex numbers for the calculations and later check that the answer has zero imaginary part.

4.7. Initial state

Calculate the initial density matrix, given the muon polarization (100%), other spin polarizations (0%) and the charge state populations (specified). For rapid charge exchange the initial state has little effect and a slightly simpler solution is obtained by starting with the equilibrium population.

4.8. Measured state

Convert the flattened initial density matrix to a sum of eigenstates. Flatten the spin polarization operator **S** and convert it to use the eigenstates as basis states.

4.9. Solution

The density matrix at time t is given from equation (3). Calculate the observable muon polarization $\langle S\rangle = \mathrm{Tr}(\rho \boldsymbol{S})$ at time t as a sum of exponential terms. Evaluate this for time t over the time range used experimentally.

There are now two ways to extract a relaxation rate or frequency shift:

(i) Evaluate $P(t)$ over a specified time interval, add weights based on the muon lifetime and statistics, and fit to a function such as $P(t) = a_0 \cos(\omega t + \phi) \exp(-\lambda t)$.

(ii) Often $P(t)$ has one dominant term (or pair of conjugate terms). Search for this largest term, and extract values for λ and ω directly.

Alternatively evaluate $P(t)$ over the same time bins as the raw data and compare directly. Additional asymmetry and background terms may have to be added.

4.10. Fitting the charge exchange parameters

The difference between predicted and experimentally measured relaxation rates and shifts is now used to adjust the initial values of charge exchange rates and the hyperfine constant, and the above calculation is re-run as required within a standard Levenberg–Marquardt-type fitting routine to obtain the optimum parameters. All longitudinal and transverse data at each temperature are included to get a consistent description of the muon dynamics at that temperature.

4.11. Functional form notes

Some terms may have 'initial amplitude' $a_0 > 1.0$ or <0 especially near 'critical damping' conditions. The terms will be found to cancel, ensuring that the final evaluated $P(t)$ always starts at 1.0 as expected. Also $\mathrm{d}P/\mathrm{d}t = 0$ at $t = 0$ unless the muon's spin itself is flipped.

4.12. Memory use

The individual state Hamiltonians have size $N = (2I_1 + 1)(2I_2 + 1)\cdots(2I_n + 1)$ in each dimension. Once flattened, the matrix **X** has size N^2 in each dimension. Joining c charge states makes X have size cN^2 in each dimension, or c^2N^4 elements.

The simple system of two spin $\frac{1}{2}$ particles and two charge states therefore requires solving a 32×32 matrix to give up to 32 complex terms in the solution.

Table 1. Fitted rates of transition between (1) neutral and (2) diamagnetic states.

T (K)	A_{hf} (MHz)	ν_{12} (μs^{-1})	ν_{21} (μs^{-1})	Neutral fraction
500	−67.0	1 732 ± 90	159 ± 15	0.084 0
500	−567.1 ± 442.0[a]	700 ± 2850	2.5 ± 3.3	0.003 54
550	1842.5	10 010 ± 400	36.1 ± 1.6	0.003 59
600	1824.0	26 280 ± 230	259.7 ± 2.6	0.009 79
700	1787.0	69 300 ± 1500	1310 ± 44	0.018 6
790	1753.7	166 600 ± 8000	5390 ± 480	0.031 3
900	1713.0	418 000 ± 46 000	22 000 ± 4900	0.050 0

[a] Hyperfine constant varied in fit.

Table 2. The calculated band gap and Fermi energy for our sample, and fitted values of the energy difference between the Mu_T^0 state and the low-lying diamagnetic state. The parameters are defined in figure 6.

T (K)	Paramagnetic fraction	E_g (eV)	kT (eV)	E_F (eV)	$E_P(T)$ (eV)	$E_{ion}(T)$ (eV)	$\Delta(T)$ (eV)
550	0.003 59	1.049 17	0.047 38	−0.563 51	−0.266 74	0.296 77	−0.100 05
600	0.009 79	1.035 00	0.051 69	−0.548 83	−0.239 14	0.309 69	−0.115 63
700	0.018 56	1.006 67	0.060 30	−0.534 95	−0.240 39	0.294 57	−0.105 82
790	0.031 34	0.981 17	0.068 05	−0.525 55	−0.235 65	0.289 90	−0.105 93
900	0.050 02	0.950 00	0.077 53	−0.514 62	−0.232 23	0.282 39	−0.104 26

5. Results

Global fits for all three observables at selected temperatures are shown in figures 5(a)–(e), giving an indication of the quality of the present model. Restricting the hyperfine constant to the Mu_T^0 value, with its temperature dependence extrapolated from values determined spectroscopically below room temperature [3], we can fit the data for 550 K and above, giving the results in table 1. In principle, free fits will give an independent determination of the hyperfine constant; in practice, our data do not extend to high enough field to do this accurately. We do confirm consistency with the extrapolated values, however, as well as with those deduced from higher-field longitudinal relaxation rates [29]. Fixing the values of hyperfine constant yields more precise fits for the dynamical parameters.

For the 500 K data set, the fit requires the hyperfine constant to be significantly smaller than that for Mu_T^0, roughly consistent with though probably greater than that for Mu_{BC}^0 (compare the first two lines in table 2). Both states may contribute here or else either the population or hyperfine constant for Mu_{BC}^0 are enhanced at a defect-related site: we return to this possibility below. The fits here use an isotropic hyperfine constant corresponding to a Mu_{BC}^0 species that is mobile or which hops locally between the four bonds around a central atom or, equivalently, that can adopt a new orientation of its symmetry axis after each charge cycle. The 550 K data could likewise be fitted slightly better using a non-zero population of both paramagnetic states, but at higher temperatures it is clear from the field dependences that transitions in and out of Mu_T^0 dominate the muon spin response. This is not to say that other paramagnetic states are unpopulated, notably Mu_{BC}^0 or excited states of Mu_T^0, but these have lower hyperfine constants and their lifetimes must be too short for them to contribute either to the relaxation or to the frequency shift.

In table 1 the rate of exit from the neutral paramagnetic state is designated ν_{12} and the entry rate as ν_{21}. Simple Arrhenius plots give their respective activation energies as 0.391 ± 0.006 eV

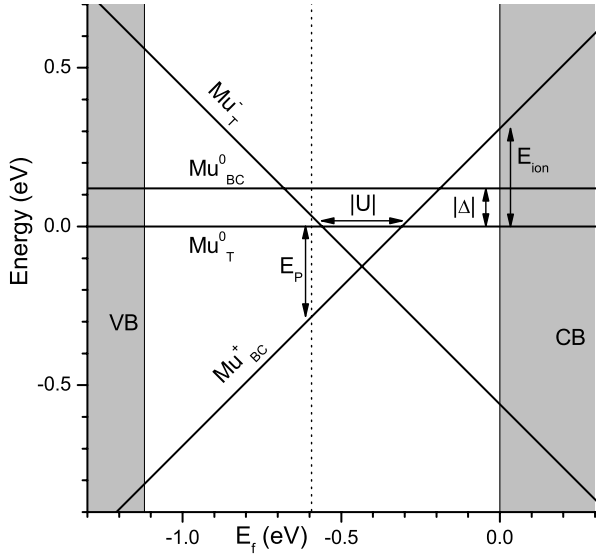

Figure 6. The energy levels for the various muon sites and charge states as a function of the Fermi energy, at 600 K.

and 0.693 ± 0.010 eV above 550 K. These are shown in figure 5. The two transition rates define the time-average occupancy or population of the dominant paramagnetic state, according to $p_0 = \nu_{21}/(\nu_{12} + \nu_{21})$, reaching 5% at 900 K as shown in figure 7[10]. In the following section we explore the expectations for and inferences from this quantity, which we call the neutral fraction.

6. Equilibrium analysis

We now assume that the system is in thermal equilibrium between all possible sites and charge states. This is rarely true for muonium studies, especially at lower temperatures. In the present case it is clearly still marginal at 500–550 K, but proves to be justified at higher temperatures by the large number of charge exchange cycles executed within the muon lifetime: the cycle rate at 600 K, for instance, is already $\nu_{12}\nu_{21}/(\nu_{12} + \nu_{21}) \sim \nu_{21} = 260\ \mu\text{s}^{-1}$.[11]

To calculate the equilibrium populations of the various muonium states, charged and neutral, we must know the Fermi energy E_F. From this point of view, the usual configuration diagram of figure 2(a) is misleading, since it is effectively drawn for E_F at the conduction band edge. We use instead the standard representation of deep-level defects, as in figure 6, where the energy of charge defects varies linearly with E_F (with a gradient equal to their charge) [44], and we have also represented the metastability of the neutral defect.

The sample is actually lightly p-type doped (boron doped with an acceptor concentration of 4.1×10^{14} cm^{-3}). In the usual notation,

$$n_\text{e} = N_\text{c} \exp(-E_\text{F}/kT),$$

[10] The Boltzmann or electron polarization contribution to the frequency shift (equation (1)) is reduced accordingly and is neglected in the fits of figure 5 and table 1.

[11] The muon spin relaxation, of course, is slow by comparison; it is not usual in μSR studies to speak of a muon spin temperature but this remains, in effect, very much lower than the lattice or electron temperature until the spin relaxation is complete.

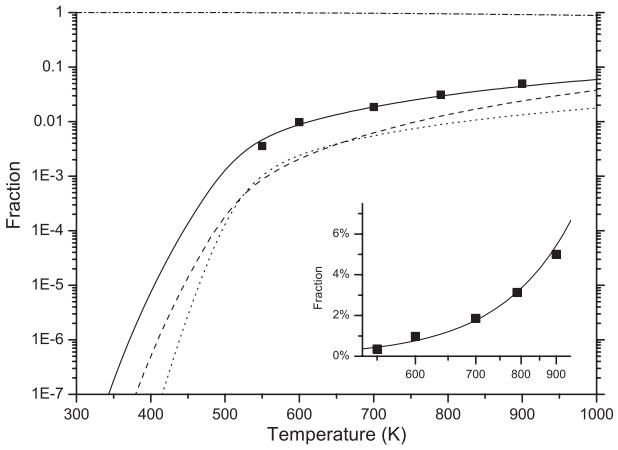

Figure 7. Equilibrium populations of the muon states as a function of temperature. The data points are our experimental results for the neutral fraction p_0, i.e. the time-average occupancy of Mu^0_T, also shown on linear scales in the inset. — · —: Mu^+_{BC}; ——: Mu^0_T; · · · · · ·: Mu^-_T; - - - -: Mu^0_{BC}; ■: fitted paramagnetic fraction.

$$n_h = N_v \exp(-E_g + E_F/kT)$$

and, for a doped semiconductor when all the donors and acceptors are ionized,

$$n_e - n_h = N_d - N_a.$$

For Si, the electrons have non-spherical symmetry, with effective mass parallel to k, $m_{el} = 0.98$ and perpendicular $m_{et} = 0.19$, and there are $M_c = 6$ equivalent minima in the Brillouin zone. The effective degeneracy of the band is therefore [41]:

$$N_c = 2m_{el}^{1/2} m_{et} M_c h^{-3} (2\pi kT)^{3/2}.$$

There are two degenerate bands of holes with $m_{h1} = 0.49$ and $m_{h2} = 0.16$, giving the degeneracy

$$N_v = 2(m_{h1}^{3/2} + m_{h2}^{3/2}) h^{-3} (2\pi kT)^{3/2}.$$

The band gap E_g is 1.12 eV at 300 K, linearly decreasing with T above 300 K (the gradient giving 1.205 eV when extrapolated to $T = 0$). The Fermi energy can be calculated for any temperature, and shows that this sample becomes intrinsic around 600 K with E_F just below the centre of the gap. For lower temperatures, E_F is closer to the valence band. We use the doped Fermi energy in the calculations below. The effect of the muons themselves as donors or acceptors, and the electron–hole pairs formed along the track, are neglected compared to the intrinsic carrier concentration.

We assume also that the donor/acceptor levels scale proportionally with E_g. (An alternative approach, which makes little difference to our conclusions, would be to assume the donor and acceptor depths locked to the respective band edges.) If there is a low-lying diamagnetic level (assumed to be Mu^+_{BC} for E_F midway in the gap or below) and all other levels are high enough in energy to be <5% populated, then we can approximate the population of Mu^0_T as

$$p_0 = \exp(-(E_{Mu^0_T} - E_{Mu^+_{BC}})/kT) N_T/N_{BC} = \exp(-E_P/kT) N_T/N_{BC}.$$

Here N_T and N_{BC} are multiplicity factors: the numbers of T and BC sites in the structure are in the ratio 1:2 for Si, but including a factor of 2 for the spin degeneracy of the T site paramagnetic state the net ratio is $N_T/N_{BC} = 1$. The quantity E_P is defined here as the energy

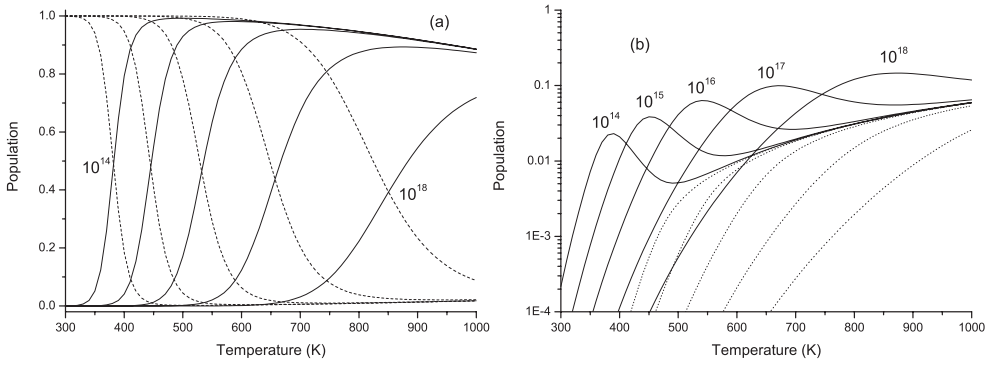

Figure 8. Equilibrium populations for various doping levels: (a) - - - -: Mu_T^- and ——: Mu_{BC}^+ for n-type doping. (b) Mu_T^0 with n-type (——) and p-type (· · · · · ·) doping.

difference between the Mu_{BC}^+ and Mu_T^0 states when the Fermi energy E_F takes its equilibrium value near mid-gap, as illustrated in figure 6. It is also useful to define $E_{ion}(T) = -E_F - E_P$ as the corresponding energy difference in the hypothetical case where the Fermi energy lies at the conduction band edge.

The resulting energy differences E_P between Mu_T^0 and Mu_{BC}^+ are shown in table 2; they exhibit a small temperature dependence consistent with the variation of the Fermi energy. Taking the single-site ionization energy of Mu_{BC}^0 to be 0.21 eV [11], scaled for the high-temperature band gap, and using the construction of figure 6, we obtain $\Delta = -0.105 \pm 0.005$ eV over the range 600–900 K. By implication, Mu_T^0 is more stable than Mu_{BC}^0 in this range, possibly indicating an inversion of the site preference from cryogenic temperatures.

We can now calculate the populations of all the states at any temperature, as in figure 7. The fraction of Mu_{BC}^0 will be around 0.2% at 600 K, independent of Δ, and decreasing at lower temperatures. The fitting of an intermittent hyperfine parameter resembling that of Mu_{BC}^0 in the 500 K data set (top two lines of table 1) suggests a longer lifetime and out-of-equilibrium population for this state at this lower temperature. This may indicate a transient pairing of muonium with a boron dopant atom, even though passivation complexes are not stable at these temperatures, or it may represent the effect of other impurities such as oxygen that are believed to catalyse the T to BC site change [42, 43]. Muons may trap into such sites for $T \leqslant 500$ K but for $T > 550$ K the probability of a muon occupying such a site at any instant is small.

It is interesting to note that for moderate n-type doping the same calculations predict that the dominant charge state should switch from Mu_T^- around room temperature to Mu_{BC}^+ at high temperature, accompanied by a peak in the neutral fraction—see figure 8. The peak value of the neutral fraction in this case would be a sensitive measure of the elusive Hubbard or Anderson parameter U.

For our sample the fractions of Mu_T^0 and Mu_T^- are comparable. We could have: (a) *in situ* ionization of Mu_T being much faster than any site changes and therefore determining the lifetime of Mu_T^0 or (b) the ionization being much slower than the change to Mu_{BC}^+. If both rates contribute to the lifetime then the relaxation can sometimes be non-exponential. The rate of transition from the lowest diamagnetic level (population >99% for $T < 600$ K) provides an upper limit to the overall relaxation rate possible, however rapidly the muon polarization may be relaxed as a result of charge cycling between the other possible states. Otherwise the field dependence of the relaxation rates is a function of the lifetime of the paramagnetic state.

7. Electron processes versus hole processes

The dominant process causing charge cycling may be either the site change from Mu_{BC}^{+} to Mu_{T}^{0}, or charge cycling in the Mu_{T} state. Consider first the site change process. From table 1 the activation energies for the transitions are

$$\begin{aligned} Mu_{T}^{0} &\rightarrow Mu_{BC}^{+} \qquad 0.391\ \text{eV}, \\ Mu_{BC}^{+} &\rightarrow Mu_{T}^{0} \qquad 0.693\ \text{eV}. \end{aligned}$$

These may be due to either electrons or holes:

$$Mu_{T}^{0} \rightarrow Mu_{BC}^{+} + e^{-}, \tag{5a}$$

$$Mu_{T}^{0} + h^{+} \rightarrow Mu_{BC}^{+}, \tag{5b}$$

$$Mu_{BC}^{+} \rightarrow Mu_{T}^{0} + h^{+}, \tag{5c}$$

$$Mu_{BC}^{+} + e^{-} \rightarrow Mu_{T}^{0}. \tag{5d}$$

Capture processes (5*b*) and (5*d*) depend on the carrier concentration and cross-sections. Processes (5*a*) and (5*c*) can be considered as having an 'activation' energy which should be no less than the corresponding ionization energy. The principle of detailed balance requires the number of muons undergoing each transition—the rate multiplied by the population—to be equal in the forward and reverse directions, so we need only analyse one direction.

From figure 6 the ionization energy for (5*a*) is $-E_{F} - E_{P} = 0.309$ eV so an activation energy of 0.391 eV is plausible for an electron ionization with an accompanying site change.

However, for process (5*c*) the hole ionization energy is $E_{P} + (E_{g} + E_{F}) = 0.726$ eV which is greater than the experimentally obtained activation energy, so we can exclude the acceptor ionization process. Therefore the charge cycling takes place by electron capture and loss.

Next consider the *in situ* ionization. This may again be due to either electrons or holes:

$$Mu_{T}^{0} \rightarrow Mu_{T}^{-} + h^{+}, \tag{6a}$$

$$Mu_{T}^{0} + e^{-} \rightarrow Mu_{T}^{-}, \tag{6b}$$

$$Mu_{T}^{-} \rightarrow Mu_{T}^{0} + e^{-}, \tag{6c}$$

$$Mu_{T}^{-} + h^{+} \rightarrow Mu_{T}^{0}. \tag{6d}$$

Again the capture processes (6*b*) and (6*d*) depend on the carrier concentration and cross-sections, and processes (6*a*) and (6*c*) can be considered as having an 'activation' energy which should be no less than the corresponding ionization energy.

From figure 6 the electron ionization energy for process (6*c*) is 0.56 eV so an activation energy of 0.693 eV is plausible for an electron ionization/capture cycle. However, the hole ionization energy for (6*a*) is about 0.5 eV which is greater than the experimentally obtained activation energy, so we can exclude the acceptor ionization process. Once again, one can conclude that the charge cycling takes place by electron capture and loss.

8. Concluding remarks: confirmation of negative U and determination of its value

Figure 6 summarizes our findings. Represented here are the same four states as account for muonium spectroscopy and dynamics up to room temperature. Allowing only for a continued variation of the Mu_{T}^{0} hyperfine constant to higher temperature we find no need to invoke additional or qualitatively different high-temperature states. We use the single-site ionization energy of Mu_{BC}^{0}, as determined from RF resonance studies below room temperature [11] and adjusted only in proportion to the temperature dependence of the band gap to fix its point of equilibrium with Mu_{BC}^{+}. Assuming this latter to be the stable ionic state under intrinsic

conditions, i.e. with the Fermi energy near mid-gap, we use our results for the neutral fraction to establish that Mu_T^0 lies higher in energy than Mu_{BC}^+ by 0.250 ± 0.02 eV. Extrapolated to room temperature, this difference becomes close to 0.3 eV.

This procedure forces us to the conclusion that, in the temperature range 600–900 K at least, Mu_T^0 lies lower than Mu_{BC}^0 by an energy $\Delta = -0.105 \pm 0.005$ eV. Extrapolated to room temperature, the equivalent difference is 0.12 eV.

Our basic supposition that Mu_{BC}^+ remains the most populated state, from room temperature up to 900 K, deserves comment. Certain computational models appear to show that proton trajectories avoid the bond-centred site at these temperatures [45] but these may be misleading, since the simulation time windows do not exceed a few picoseconds (and are mostly much shorter), whereas our diamagnetic state lifetimes vary between 40 ps at 900 K and 4 ns at 600 K. The breakdown of adiabaticity is not something which sets in abruptly at high temperature—it may already be manifest in the T to BC barrier which assures the metastability of muonium at cryogenic temperatures. On the other hand, Mu_T^0 is already found to be more stable than Mu_{BC}^0 in a calculation which introduces a double adiabatic approximation, in which electrons, muons or protons, and host nuclei are separately decoupled [46]. It may also be that the effective barrier height increases with temperature [25] and that vibrational enthalpies modify or even invert the stabilities of the two sites.

This reordering of the T and BC levels implies a redefinition of donor and acceptor levels, at least at high temperature. The new values are given by the appropriate intersections in figure 6. Accepting the RF-μSR results of 0.56 eV for the single-site ionization energy of the negative ion, Mu_T^-, and of 0.21 eV for that of the bond-centred neutral, Mu_{BC}^0 [11], we define the donor level as lying below the conduction band edge by $E_D = 0.21 + 0.12 = 0.34$ eV and find the acceptor level to lie essentially at mid-gap, as was noted at lower temperature for hydrogen [18]. In conclusion, we confirm negative-U behaviour and estimate this elusive quantity to be

$$U = 0.21 - 0.56 + 0.12 = -0.23 \text{ eV}.$$

The Mu(+/−) pinning level, where Mu_{BC}^+ and Mu_T^- are in equilibrium, and where the Fermi energy would be pinned in the hypothetical case where muonium centres are in abundance, dominating shallow dopants, lies above mid-gap, about 0.42 eV below the conduction band edge.

References

[1] Stutzmann M and Chevallier J (ed) 1990 *Hydrogen in Semiconductors* (Amsterdam: North-Holland) ISBN 0-444-89138-2
[2] Brewer J H *et al* 1973 *Phys. Rev. Lett.* **31** 143
[3] Patterson B D 1988 *Rev. Mod. Phys.* **60** 69
[4] Kiefl R F and Estle T L 1991 *Physica* B **170** 33 (reprinted in [1])
[5] Chow K H 1997 *Hyperfine Interact.* **105** 285
[6] Cox S F J and Symons M C R 1986 *Chem. Phys. Lett.* **126** 516
[7] Estle T L, Estreicher S and Marynick D S 1987 *Phys. Rev. Lett.* **58** 1547
[8] Kiefl R F *et al* 1988 *Phys. Rev. Lett.* **60** 224
[9] Kreitzman S R *et al* 1995 *Phys. Rev.* B **51** 117
[10] Lichti R L 1995 *Proc. R. Soc.* A **350** 323
[11] Hitti B *et al* 1999 *Phys. Rev.* B **59** 4918
[12] See for instance Madelung O 1996 *Semiconductors: Basic Data* (Berlin: Springer)
[13] Gil J M *et al* 2001 *Phys. Rev.* B **64** 075205
[14] Cox S F J 2003 *J. Phys.: Condens. Matter* **15** R1727
[15] Van de Walle C G *et al* 1989 *Phys. Rev.* B **39** 10791
[16] Chow K H *et al* 1995 *Phys. Rev.* B **51** 14762

[17] Chow K H *et al* 2003 *Physica* B **340–342** 280
[18] Bonde-Nielsen K *et al* 1999 *Phys. Rev.* B **60** 1716
[19] Estreicher S K 2003 *Hydrogen in Materials and Vacuum Systems* ed G R Myneni and S Chattopadhyay (New York: AIP) p 40 0-7354-0137-3/03
[20] Gorelkinskii Yu V and Nevinnyi N N 1987 *Sov. Tech. Phys. Lett.* **13** 45
see also Gorelkinskii Yu V and Nevinnyi N N 1991 *Physica* B **170** 155 (reprinted in [1])
[21] Herring C *et al* 2001 *Phys. Rev.* B **108** 222
[22] Hourahine B 2000 *Thesis* University of Exeter
[23] Cox S F J 1995 *Phil. Trans. R. Soc.* A **350** 227
[24] Chu C H and Estreicher S K 1990 *Phys. Rev.* B **42** 9486 plus references therein
[25] Sanati M and Estreicher S K 2003 *Physica* B **340–342** 630
[26] Cottrell S P *et al* 2003 *Physica* B **326** 260
[27] Storchak V G *et al* 1997 *Phys. Rev. Lett.* **78** 2835
[28] Eshchenko D G *et al* 2002 *Phys. Rev. Lett.* **89** 226601
[29] Chow K H *et al* 1993 *Phys. Rev.* **47** 16004
[30] Chow K H *et al* 2000 *Phys. Rev. Lett.* **84** 2251
[31] Senba M 2001 *J. Phys. B: At. Mol. Opt. Phys.* **34** 4437
[32] Iwanowski M *et al* 1994 *Hyperfine Interact.* **86** 681
[33] Kadono R *et al* 1994 *Phys. Rev. Lett.* **73** 2724
[34] Kadono R, Macrae R M and Nagamine K 2003 *Phys. Rev.* **68** 245204
[35] http://lmu.web.psi.ch/facilities/gps/gps.html
[36] Cox S F J *et al* 2001 *J. Phys.: Condens. Matter* **13** 2155
[37] Hitti B and Kreitzman S R 2003 *Physica* B **326** 178
[38] Cox S F J *et al* 2003 *Physica* B **340–342** C641
[39] Senba M 1991 *J. Phys. B: At. Mol. Opt. Phys.* **24** 3531
[40] Gorelkin V N *et al* 2000 *Physica* B **289/90** 585
[41] Smith R A 1978 *Semiconductors* (Cambridge: Cambridge University Press)
[42] Estreicher S K, Park Y K and Fedders P A 1996 *Early Stages of Oxygen Precipitation in Silicon* ed R Jones (Dordrecht: Kluwer) p 179
[43] Bonde Nielsen K *et al* 2002 *Phys. Rev.* B **65** 175205
[44] See, for example Pantelides S 1986 *Deep Level Centers in Semiconductors—a State of the Art Approach* (London: Gordon and Breach)
[45] Buda F *et al* 1989 *Phys. Rev. Lett.* **63** 294
[46] Porter A R, Towler M D and Needs R L J 1999 *Phys. Rev.* B **60** 13534